Accepted Manuscript

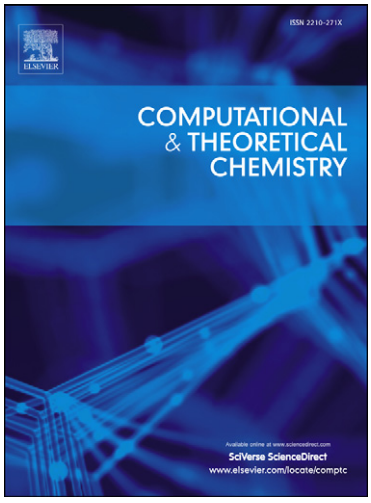

Metal salts reduction during parylenes polymerization

Maciej Bobrowski

PII: S2210-271X(12)00189-2
DOI: 10.1016/j.comptc.2012.03.021
Reference: COMPTC 691

To appear in: *Computational & Theoretical Chemistry*

Received Date: 22 October 2011
Revised Date: 18 March 2012
Accepted Date: 25 March 2012

Please cite this article as: M. Bobrowski, Metal salts reduction during parylenes polymerization, *Computational & Theoretical Chemistry* (2012), doi: 10.1016/j.comptc.2012.03.021

Metal salts reduction during parylenes polymerization

Maciej Bobrowski[a,b,1]

[a] *Faculty of Technical Physics and Applied Mathematics, Gdansk University of Technology, Narutowicza 11/12, 80-233 Gdansk, Poland*

[b] *Academic Computer Center in Gdansk TASK, Technical University of Gdansk, ul. Narutowicza 11/12, 80-233 Gdansk, Poland*

Abstract

Recently it was discovered that some metals and some metal salts quench the polymerization of poly-para-xylylenes (also known as parylenes) [Vaeth et al., *Chem. Mater.*, 2000, **12**, 1305–1313]. The inhibitions were found to be dependent on the metal type. On the other hand, it is known that the polymerization mechanism of parylenes is of radical type [Smalara et al., *J. Phys. Chem. A*, 2010, **114**, 4296–4303, Errede et al., *Q. Rev. Chem. Soc.*, 1958, **12**, 301–320] and no catalyst or solvent is required in this process. In the present work we postulate that the reaction between parylene and metal salts can go through one-electron reduction of metal salts by radical parylene chains. We also consider the role of monomers in this type of reactions and propose a stechiometric notation for the reductions. Thermodynamical barriers were found by means of DFT calculations with two different functionals and various basis sets and to estimate the changes of the enthalpy and Gibbs free energy we computed the translational, rotational and vibrational contributions to the partition functions of the substrates and products. Additionally, water solvent effects have been appraised in the PCM model and the energy relations were compared to those calculated for gas- phase reactions. It turned out that in the case of metal salts where an appropriate reduction of metal characterizes sufficiently high positive value of standard redox potential, the reaction is thermodynamically favorable. Moreover, one can find that within some domain there is a tendency that the higher the potential the more stable products

Keywords: CVD, parylen, polymerization quenching, metal salt reduction

Introduction

Poly(chloro-para-xylylenes) whose trade name is parylenes have excellent qualities, both physical and chemical. This family of polymers work generaly as moisture and dielectric barriers in various applications harnessing surface covering and yielding interface barriers. So, the majority of parylene used is deposited as passivation barriers protecting devices or other parts from environment involving water, chemicals or electrical field. It's completely clean technology utilizing no activators, catalysts, solvents, etc. However, recently independent groups[1, 2] found that the same technology can be used with liquid substrates without affecting the shape of the liquid. Not surprisingly, their properties gained interest in the introduction of useful functionalities leading to novel materials and adapted processes.

The mechanisms of polymerization process of parylene polymers are generally well-known. Since 1947 when Szwarc synthesized the parylene[3] for the first time there have been many experimental and theoretical attempts in finding of the polymerization mechanism of this family of polymers. The yield of the Szwarc process, namely rapid flow pyrolysis of p-xylene under reduced pressure, was very low (did not exceeded a few percent) but in 1966 at Union Carbide

Email address: mate@mif.pg.gda.pl (Maciej Bobrowski)

[1] Tel: + 48 58 3471235, Fax: + 48 58 3472821

Gorham developed a better method[4] where cyclo-di-p-xylylene (CDPX, [2,2]para- cyclophane) was used as a substrate for the polymerization. Accordingly to Gorham's report, 100% of the CDPX were cracked onto monomers which next took part in the polymerization. It was not until 1958 when Errede and Szwarc proposed qualitative description of the mechanism[5]. In compliance with their publication, the polymerization process initializes from reaction of two monomers with a sufficiently high kinetic energy. The product - di-p-xylylene (DPX) - has biradical nature and can react with another monomer leading to biradical trimer - tri-p-xylylene (TPX), and so on. The process requires neither solvents nor catalysts and thus allows to produce

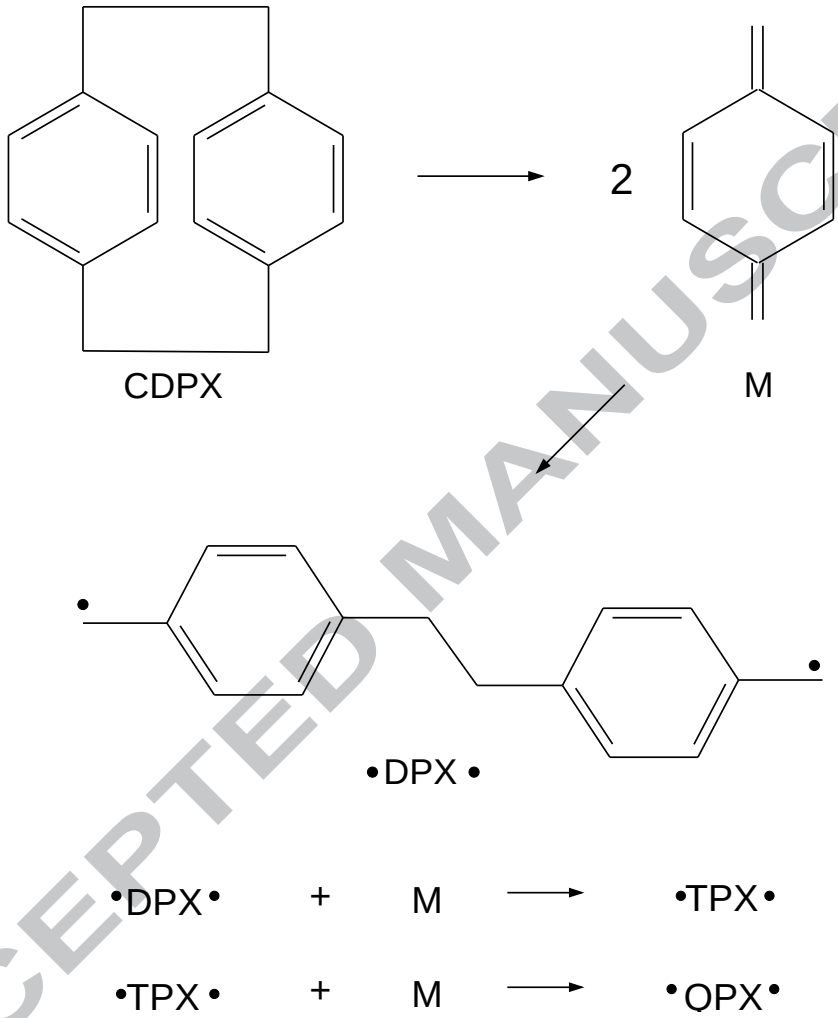

Figure 1. Scheme of cracking of the cyclo-di-p-xylylene into monomers in the pyrolysis process, initiation and first propagation steps (up to tetramer (the QPX)) of polymerization

non-polluted thin films of polymer over a wide range of materials, including liquids with uniform replication of the shape of its droplets[1]. Moreover, the polymerization itself occurs at room temperature which effectively spreads its applications onto electronics, optics, medicine, aviation and the automotive industry [6–12]. Current technological applications, including production of semiconductors and small electronic components, corrosion control, coating of circuit boards and production of dry lubricants, and recently also biomedical solutions [9, 13, 14], are well completed by new trends related to parylenes functionalization. To do this, two main threads are being developed simultaneously. One is the modification of [2,2]para-cyclophane before the polymerization[15–18]. After following vapor deposition one can obtain functionalized chains of parylene but this method requires modification of technological parameters and the resulting polymers basically posses different properties. Also, the chains are strongly changed due to

different structure of monomers and therefore the morphology of parylene layers is different. The second method includes using suitable substrates which are capable of reacting with non-modified parylene during the CVD polymerization. This kind of process does not require any technological modification and the product forms a tiny layer chemically connected to the parylene. The mody-layer can further be used as a bridge in various functionalizations, depending on requirements[19, 20].

Recently measured UV-Vis, IR and Raman spectra explicitly indicate chemical functionalization of parylene layer after the deposition on liquids containing double-bond molecules[19]. The experimental report on the reactivity during CVD was followed by the theoretical description of the most probable corresponding mechanisms[21, 22]. Also, the most important factors influencing the reactivity rates were taken into account. Chemical functionalization of the parylene during the CVD was also observed in the case of other types of liquids, namely in the case of acrylate-based molecules. The functionalization yields reactive electrophilic films that can be further modified by using simple nucleophilic substitutions like amidation[20].

Modification of the parylene structure without chemical functionalizations was also investigated [23–25]. In 2007 and later on Cetinkaya and coworkers[18, 24, 26] proposed a method for management of spatial organisation of parylene structures during CVD. They demonstrated a simple and effective way of fabrication of structured polymers by oblique angle deposition. The parylene's morphology control was simply achieved by manipulating the substrate rotation. Non-mechanical ways, i.e. chemical realization of more selective growth during the CVD also meet with interest[14, 25, 27, 28]. In 2000 Vaeth and Jensen[25] used various metals, metal salts and organometallic complexes and discovered that depending on the metal used they can inhibit the deposition on the substrate. Moreover, they discovered that when the metal initially inhibits polymer growth, the morphology of parylene layer has significantly larger grains, indicating fewer nucleation sites. As the Vaeth and Jensen mentioned, the type of metal influences the rate of quenching of the polymerization. In their work they suggested that between metal or metal salts and parylene there was some kind of interaction which caused quenching of polymerization. However, they did not propose any possible scenario, instead they focused on the visual effects of the process in the polymer layer. Recently Lahann and coworkers used a thin iron layer as an inhibitor for chemically selective growth of parylene and fabricated elastomeric stamps. After that, they removed the thin iron layer with an acidic solution[27]. Recent theoretical studies on some plausible scenarios of reactions between polymerizing parylene and titanium dioxide as well as gold surfaces were published by Vasenkov[29]. However, Vasenkow didn't pick up on why the metal salts can quenche parylens polymerization.

In the present work we postulate that the reactions between parylene and metal salts go through one-electron reduction of metal cations by means of radical chains of parylene. This type of reaction strongly depends on the metal used. In literature there were many evidences supporting the reduction. First of all one has to mention that metal ions with appropriate redox potentials can undergo one-electron reductions with radicals and there are publications as far back as the 50s describing studies of radical polymerizations of vinyl monomers by metal ions. Preparation and synthesis of nanoparticles might go through the reaction of organic radicals with metal salts[30]. Sulfite radicals can undergo redox reactions where the organic radicals are involved both as substrates and as products[31]. The radical $SO_2^{-\cdot}$ itself is in turn known to be a highly reactive one-electron reductant and reduces metalloporphyrins containing Fe(III), Co(III), and Mn(III) as well as wide variety of electron-transfer proteins (radical reactions). Aqueous polymerization of a number of vinyl monomers can be easily initiated by means of ferrous-bromate mixture. Pramanick and Palit found that neutral salts can depress vinyl polymerization, while they even estimated that the overall activation energy is 7.47 kcal/mole[32]. Niemi and coworkers reported that direct oxidation of 3-alkylthiophenes using ferric chloride ($FeCl_3$) leads to high molecular weight poly(3-alkylthiophenes). Their studies show that the $FeCl_3$ must exist in the reaction mixture to be active as an oxidant in the polymerization. Moreover, they concluded, that the synthesis might proceed through a radical mechanism[33]. It's also a common

knowledge, that in Fenton reaction (known from over 100 years) we use hydrogen peroxide and get hydroxyl radical. The hydroxyl radicals can easily diffuse through cell membranes and react with lipids, mainly with phospholipids (OH• + R = HOR•). The radical product is eable to reduce Fe^{3+} to Fe^{2+}.

Since the mechanism of plausible reactions between the metals salts and growing parylene chains is yet unknown, one can reliably predict products of such reactions if only the stechiometricity is kept. We consider either the participation of monomers in the reduction, instead of the radicals. Errede and Szwarc[5], as well as Fortin and Lu[34], Bowie and Zhao[35] suggested that in first phases of the CVD the p-xylylene monomers adhere on the substrates and group into clusters, while the polymerization starts later. It is also obvious that monomers posses higher mobility in comparison to the oligomers or any longer chains which means they should posses larger amount of kinetic energy which makes their diffusion easier. Smalara et al.[36] found energy diagrams of all exhibited steps at the polymerization path which shed more light at the polymerization mechanism. They convincingly explained why existing chains grow faster than new chains are created: the kinetic energy barriers for initialization reactions is a few times higher than the one in the case of propagation reactions. However, monomers are involved in both of these reactions. Therefore, it seems likely that the monomers might play a role in the one-electron reduction of metal salts and we involve them in the calculations as well and try to explain their role.

Methods

Model substrates and products

Various metals were used to model the energetics of the reactions. They were chosen arbitrarily but the limitation was to choose only those metals for which the standard redox potential corresponds to one-electron or two-electron reductions and that after reactions the reduced form is still a cation, not an uncharged atom. For 13 reactions that were chosen see table1.

Table 1. Electronic configurations of selected metal cations before and after one-electron and two-electron reductions and corresponding values of standard redox potentials.

		One-electron reduction		
No.	Me^{n+} / $Me^{(n-1)+}$	Me^{n+} config.	$Me^{(n-1)+}$ config.	E^0 [V]
1	Ag^{2+} / Ag^{+}	$[Kr]4d^{9}5s^{0}$	$[Kr]4d^{10}5s^{0}$	+1.98
2	Co^{3+} / Co^{2+}	$[Ar]3d^{6}4s^{0}$	$[Ar]3d^{7}4s^{0}$	+1.81
3	Mn^{3+} / Mn^{2+}	$[Ar]3d^{4}4s^{0}$	$[Ar]3d^{5}4s^{0}$	+1.51
4	Fe^{3+} / Fe^{2+}	$[Ar]3d^{5}4s^{0}$	$[Ar]3d^{6}4s^{0}$	+0.77
5	Cu^{2+} / Cu^{+}	$[Ar]3d^{9}4s^{0}$	$[Ar]3d^{10}4s^{0}$	+0.15
6	Ti^{4+} / Ti^{3+}	$[Ar]3d^{0}4s^{0}$	$[Ar]3d^{1}4s^{0}$	0.00
7	V^{3+} / V^{2+}	$[Ar]3d^{2}4s^{0}$	$[Ar]3d^{3}4s^{0}$	-0.26
8	Ti^{3+} / Ti^{2+}	$[Ar]3d^{1}4s^{0}$	$[Ar]3d^{2}4s^{0}$	-0.37
9	Cr^{3+} / Cr^{2+}	$[Ar]3d^{3}4s^{0}$	$[Ar]3d^{4}4s^{0}$	-0.41
10	In^{3+} / In^{2+}	$[Kr]4d^{10}5s^{0}5p^{0}$	$[Kr]4d^{10}5s^{1}5p^{0}$	-0.49
		Two-electron reduction		
No.	Me^{n+} / $Me^{(n-2)+}$	Me^{n+} config.	$Me^{(n-2)+}$ config.	E^0 [V]
1	Pb^{4+} / Pb^{2+}	$[Xe]4f^{14}5d^{10}6s^{0}6p^{0}$	$[Xe]4f^{14}5d^{10}6s^{2}6p^{0}$	+1.67
2	Sn^{4+} / Sn^{2+}	$[Kr]4d^{10}5s^{0}5p^{0}$	$[Kr]4d^{10}5s^{2}5p^{0}$	+0.15
3	In^{3+} / In^{+}	$[Kr]4d^{10}5s^{0}5p^{0}$	$[Kr]4d^{10}5s^{2}5p^{0}$	-0.44

Additionally, to avoid doubts, in the case of all the metals the electronic configuration before and after the reduction was build for high- and low-spin systems. It was therefore possible

to compare energies of various-multiplicity salts and definitely choose only those for which the energy was lowest. Unless the Hund's rule is observed in this case various basis sets and methods used will contort the relations. For such systems the energetics of high- and low-spin systems was calculated as described in the next subchapter.

Three biradical substrates: dimer, trimer and tetramer represented the short parylene chains. They are the smallest molecules yet available for quantum calculations. Additionally, the closed-shell monomer (p-xylylene) was involved in exchange for biradical substrates hoping to define its role in this type of reductions. In all salts the anion was chosen as chloride while the biradical substrates were treated as triplet and the monomer as singlet closed-shell molecule[21, 22].

Quantum-chemical computations

Geometries of all separate substrates and products were optimized by using both density functional theory (DFT) and one-determinant Hartree-Fock (R(O)HF) method, for comparison. The inclusion of dynamic correlation effects in the DFT avoided additional overheads as in the post Hartree-Fock methods. However, one could assume that such effects on one hand would decrease energy relations in studies of the mechanisms of chemical reactions but would play a smaller role while studying only energy relations between substrates and products of reactions. For comparison, two different density functionals were used in the DFT calculations, the BHHLYP[37] exchange/correlation which comprises 50% HF plus 50% B88, with LYP correlation as well as B3LYP[38–40] which is a hybrid of 5 functionals, namely Becke, Slater and HF exchange, and LYP + VWN5 correlation. The BHHLYP and B3LYP density functionals were applied many times with success when metals and non-metals were considered[41–43].

Various basis sets were used both in HF and DFT calculations aiming at best description of the metal atom. An all-electron 6-31G(d)[44–46] and 6-31+G(d)[47] were used for carbon, chlorine and hydrogen atoms while for metals - three different pseudopotentials were used: SBKJC, LANL2DZ and MCP NOSeC VTZP. The SBKJC[48–50] and LANL2DZ[51–53] are examples of effective core potentials (ECP) which generates nodeless valence orbitals (they are known to cause too large exchange integrals in ECP). The MCP NOSeC VTZP[54–60] is an example of model core potential (MCP) where the coefficients and exponents of contracted Gaussian-type functions (cGTFs) were optimized to minimize the difference from natural orbitals (NOSeC, natural orbital based segmented CGTF). The MCP produces valence orbitals with the correct radial nodal structure.

Geometry optimizations were performed for separate substrates and products. After the location of local minimas the differences $E_{product} - E_{substrate}$ were calculated and are further referred to as relative energies or ΔE. The calculations were performed for gas-phase as well as in the presence of solvent modeled as polarizable continuum within the PCM theory. In the PCM method a solute is placed in a cavity formed by a union of spheres centered on each atom. The chosen solvent was water whereas the spheres defining the cavity were taken to be 1.2 times the van der Waals radii.

To estimate the changes of the enthalpy (ΔH) and Gibbs free energy (ΔG; this quantity is directly related to the equilibrium constant of a reaction) of the reactions studied, we computed the translational, rotational and vibrational contributions to the partition functions of the substrates and products (accordingly to the harmonic approximation approach). While the translational contributions are the same for substrates and products when the system under study is treated as a whole, we do not consider them at all in the calculations. The rotational and vibrational partition functions and the respective contributions to ΔH and ΔG were computed following the Hessian calculation for each of the system studied.

All calculations were carried out using either GAMESS[61] and Gaussian'03[62] programs.

Results and Discussion

Low- and high-spin states of metal salts

The comparison of energetics of high- and low-spin states of metal salts is presented in Table 2. The number of states depends on the number of electrons at valence energy levels and in the case of silver, copper and indium there is only one possible electronic configuration for each oxidation state, however for comparison they were also put in this table. The energies were calculated as differences between the low-spin (l) and the high-spin (h) state for each metal cation ($\Delta E = E_l - E_h$). As shown in table 2, all relative energies are positive, sometimes relatively high. Comparing the ΔE for various spin-states of the same atoms one can see that the higher the differences between multipilicites of same cations the higher the relative energy. It is also well visible that the lowest energies are associated with the highest spins while the highest energies are associated with the lowest spins (it is best visible in the case of copper III and iron III chlorides where there were three different spin states). Therefore, one can reliably state that in all cases the high-spin states are the most stable configurations. This is well correlated with many experiments, where the high-spin configurations were the most stable in comparison to low-spin configurations [63–67].

Since the results and the literature data lead to the same conclusions, we are confident that the high-spin states metal salts are the lowest-energy configurations and we shall use them further in the calculations of energetics of one- and two-electron reductions of the metal salts by means of radical oligomers and by closed-shell monomers of parylene.

Table 2. Relative energies (kcal/mol) of low-spin (l) and high-spin (h) states ($\Delta E = E_l - E_h$) of selected metal salts. The calculations were performed at the DFT level with the use of BHHLYP potential and MCP NoSeC VTZ basis set on metal and 6-31G(d) on chlorine atoms. The values in parenthesis correspond to results obtained with the use of the PCM solvation model.

No.	Metal type	${}^{X}Me^{n+}$	ΔE [kcal/mol]	${}^{X}Me^{(n-1)+}$	ΔE [kcal/mol]
1	Ag	${}^{2}Ag^{2+}$	0	${}^{1}Ag^{+}$	0
2	Co	${}^{5}Co^{3+}$	0	${}^{4}Co^{2+}$	0
		${}^{3}Co^{3+}$	19.16 (20.55)	${}^{2}Co^{2+}$	53.99 (44.08)
		${}^{1}Co^{3+}$	41.94 (42.28)		
3	Mn	${}^{5}Mn^{3+}$	0	${}^{6}Mn^{2+}$	0
		${}^{1}Mn^{3+}$	63.29 (63.15)	${}^{2}Mn^{2+}$	125.96 (128.70)
4	Fe	${}^{6}Fe^{3+}$	0	${}^{5}Fe^{2+}$	0
		${}^{4}Fe^{3+}$	10.03 (7.40)	${}^{1}Fe^{2+}$	92.99 (95.19)
		${}^{2}Fe^{3+}$	39.10 (34.89)		
5	Cu	${}^{2}Cu^{2+}$	0	${}^{1}Cu^{+}$	0
6	Ti	${}^{1}Ti^{4+}$	0	${}^{2}Ti^{3+}$	0
7	V	${}^{3}V^{3+}$	0	${}^{4}V^{2+}$	0
		${}^{1}V^{3+}$	20.72 (22.06)	${}^{2}V^{2+}$	29.14 (29.48)
8	Ti	${}^{2}Ti^{3+}$	0	${}^{3}Ti^{2+}$	0
				${}^{1}Ti^{2+}$	13.48 (13.79)
9	Cr	${}^{4}Cr^{3+}$	0	${}^{5}Cr^{2+}$	0
		${}^{2}Cr^{3+}$	35.21 (36.22)	${}^{1}Cr^{2+}$	114.95 (119.07)
10	In	${}^{1}In^{3+}$	0	${}^{2}In^{2+}$	0

The reduction

Stechiometric notation of reactions studied is presented in fig. 2. The reactions A and C correspond to the one-electron reduction where the chlorine atom (7 valence electrons) is

A. $\mathbf{M + MeCl_n \longrightarrow {}^{\bullet}MCl + MeCl_{n-1}}$

B. $\mathbf{{}^{\bullet}MCl + MeCl_n \longrightarrow MCl_2 + MeCl_{n-1}}$

C. $\mathbf{{}^{\bullet}YPX^{\bullet} + MeCl_n \longrightarrow {}^{\bullet}YPXCl + MeCl_{n-1}}$

D. $\mathbf{{}^{\bullet}YPXCl + MeCl_n \longrightarrow YPXCl_2 + MeCl_{n-1}}$

E. $\mathbf{M + MeCl_n \longrightarrow MCl_2 + MeCl_{n-2}}$

F. $\mathbf{{}^{\bullet}YPX^{\bullet} + MeCl_n \longrightarrow YPXCl_2 + MeCl_{n-2}}$

Figure 2. Stechiometric notation of one- and two-electron redox reactions. The reactions A-D correspond to one-electron metal salts reductions, while the reactions E-F correspond to simultaneous two-electron reductions. M stands for monomer substrate (i.e. closed-shell p-xylylene molecule), while the Y stands for dimer, trimer and tetramer, the oligomers

transferred to the organic reactant while oxidation level of the metal cation decreases. In the case of closed-shell monomer as well as in the case of diradicals the organic product becomes a radical doublet, i.e. one end of the molecule remains still active and can further take part in the polymerization or again in the reduction. The reactions B and D represent the second-step one-electron reduction of the metal salt, where the organic reactant becomes a closed-shell product which is therefore inactive neither in the reduction nor in the polymerization. The reactions E and F correspond to the hypothetical two-electron reduction, where two chlorine atoms are transferred simultaneously to the organic reactant. After that, the oxidation level of the metal cation decreases and the organic molecule becomes inactive.

In the following sections we shall consider both one-electron and two-electron reduction separately. In the former case we considered the two-step reduction, i.e. the two time one-electron reduction of the salts but with different reductors: first with the biradical triplets and in next step - with radical doublets.

One-electron reduction

Relative energies ($E_{products}$ - $E_{substrates}$) of the reductions calculated for separate systems are assembled for the first-step and for the second-step in table 3. For each reaction both the closed-shell monomer, as well as the diradical dimer, trimer and tetramer were used as organic reactants. It therefore allowed to read the role of monomers and oligomers in the reduction and to check differences between energies when radical chains of different length played role. As it was described and expounded in previous section only the high-spin configurations of all the salts studied were taken into account (see table 2). The data assembled in table 3 explicitly reveals that in the cases of metal salts for which the corresponding one-electron reduction potential is positive the thermodynamical barrier is negative. The barriers collected in table 3 are grouped against basis sets and methods used, and the comparison is additionally presented in figure 3. For silver, cobalt, manganese, iron, copper and titanium IV chlorides the barriers are significantly negative, except in the case when the Hartree-Fock level of theory and the MCP basis set were applied. Namely, in this case the barrier for the reduction of copper

II chloride was positive. Moreover, the general trend could be observed for some latitude - the higher the potential the lower thermodynamical barrier which in turn indicates that if only the one-electron reduction is characterised by sufficiently high standard redox potential the reaction is thermodynamically likely. However, such a conclusion should not be inferred for the negative potential bracket where one can see discrepancies. For titanium III and vanadium chlorides the relation seems to work yet, but for chromium chloride ($E_0 = -0.41$ V) the relation is inverse and the thermodynamical barrier becomes negative. The relative energies for second-step one-

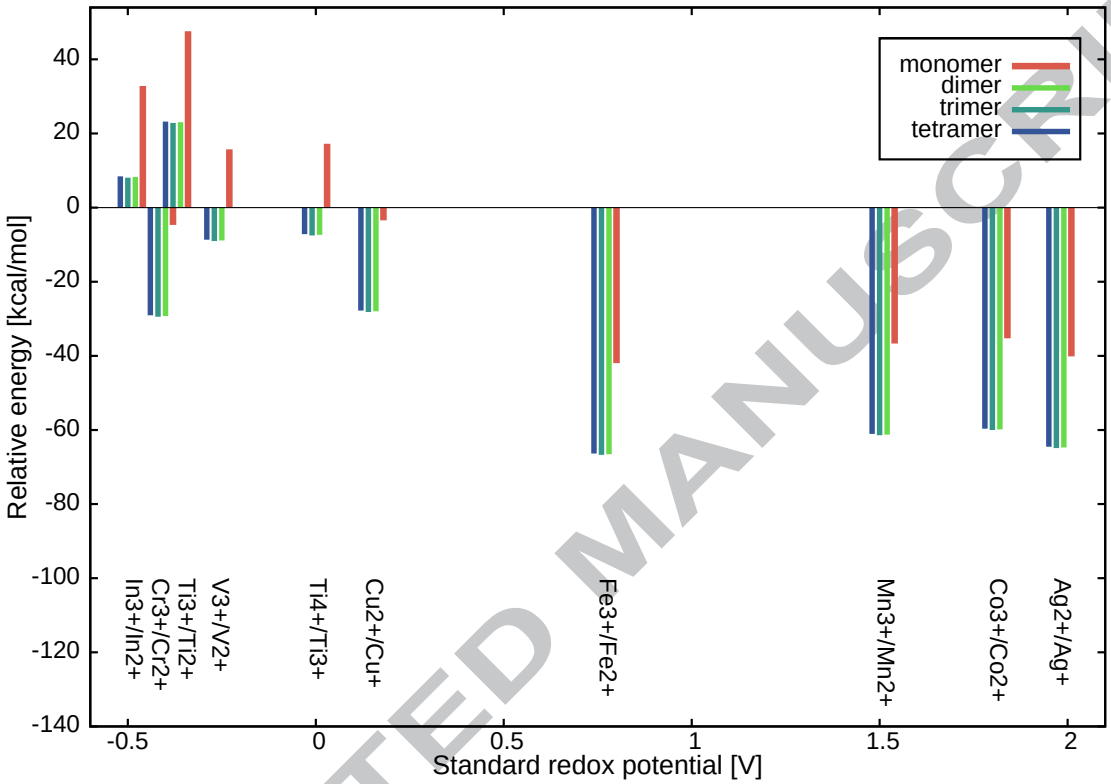

Figure 3. Thermodynamical barriers of first-step one-electron reduction by closed-shell monomers and biradical oligomers. The values correspond to results obtained for the MCP basis set applied for metals (see table 3).

electron reduction are collected also in table 3 while graphical comparison is in figure 4. One could observe a general tendency that in the case of oligomers the energy realations are almost identical to those found for the first-step reductions, while in the case of monomers the energies are shifted up by more or less constant value for almost all metal species. It is therefore likely that the only factor which plays a role in the reactions which involve radicals is the metal type and the two active radical ends of the chains work independently. It is withal obvious that the one-electron reduction of metal salts by biradical reactants in two steps can entirely quench the polymerization. This, in turn, is in good agreement with the work of Vaeth and coworkers [25] who found that some metal salts and metals can entirely quench the polymerization.

The analysis of the ΔE revealed that the reactions which involved the p-xylylene (the monomer) reactant were characterized by significantly higher thermodynamical barriers. For each salt the difference is shifted by more than 20 kcal/mol at all levels of theory (i.e. using either Hartree-Fock and DFT methods and all types basis sets) in comparison to the barriers found for biradical reactants. Moreover, the energy relations are very similar in the case of biradical reactants, regardless of length of the oligomers. One could therefore conclude that the first-step one-electron reduction should be significantly favorized in the case of radical chains no matter what length the chains grew up to during the polymerization. The case of worse

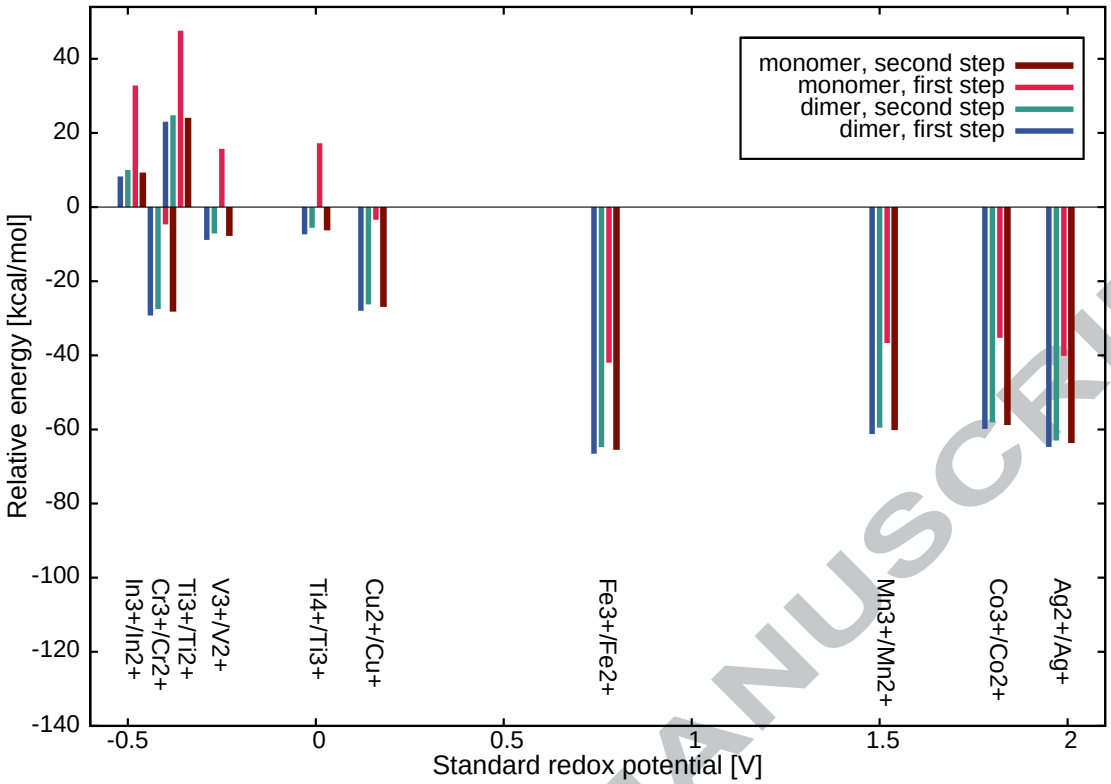

Figure 4. Comparison of the eneregtics of first- and second-step one-electron reduction by closed-shell monomers and biradical di-p-xylylene (the dimer). The values correspond to results obtained for the MCP basis set applied for metals (see table 3).

reactivity of p-xylylens in comparison to radical triplet-state oligomers is even more interesting. Recently it was proven that the ground electronic state of the p-xylylene is closed-shell singlet, while it is triplet and singlet open-shell states that are much less stable [22]. The one-electron reduction of metal salts involving closed-shell p-xylylene molecules lead to open-shell doublets which are much less stable. Similarly, on could expect that the second-step one-electron reduction leading to the singlet closed-shell organic product is much more favored in comparison to the reactivity of p-xylylens. Indeed, the energy differences did not contort this assumption (see fig. 4).

Table 3. Hartree-Fock and DFT relative energies (kcal/mol) of first-step and sescond-step one-electron reduction of metal salts by closed-shell p-xylylene (MO) and biradical di-p-xylylene (DPX), tri-p-xylylene (TR) and tetra-p-xylylene (TE) calculated for gas phase (in parenthesis) and for model of water (PCM).

Me^{n+} / $Me^{(n-1)+}$	E^0 [V]	S	HF SBKJC	RBHHLYP SBKJC	HF MCP[a] 6-31G(d)	RBHHLYP MCP[a] 6-31G(d)	UB3LYP LANL2DZ[b] 6-31+G(d)
Ag^{2+} / Ag^{+}	+1.98	MO	-28.95	-31.82	-35.90	-40.15	-28.98
			(-38.59)	(-23.17)	(-38.32)	(-32.45)	(-18.24)
		DI	-39.01	-51.84	-49.64	-64.72	-50.66
			(-48.16)	(-42.85)	(-54.14)	(-56.95)	(-64.72)
		TR	-38.99	-51.51	-47.94	-64.89	-49.40
			(-48.17)	(-42.75)	(-54.16)	(-56.86)	(-45.97)
		TE	-38.70	-51.91	-51.85	-64.53	-50.58
			(-48.17)	(-42.79)	(-54.30)	(-65.93)	(-39.85)
Co^{3+} / Co^{2+}	+1.81	MO	-28.31	-7.69	-32.37	-35.28	-17.73

			(-24.01)	(-4.64)	(-31.68)	(-32.97)	(1.87)
		DI	-38.36	-27.72	-46.11	-59.84	-39.41
			(-33.57)	(-24.32)	(-47.50)	(-57.47)	(-59.84)
		TR	-38.35	-27.38	-44.42	-60.02	-38.15
			(-33.59)	(-24.22)	(-47.52)	(-57.37)	(-25.86)
		TE	-38.06	-27.78	-48.33	-59.66	-39.34
			(-33.59)	(-24.25)	(-47.66)	(-66.45)	(-19.74)
Mn^{3+} / Mn^{2+}	+1.51	MO	-80.90	-39.53	-82.36	-36.68	-41.03
			(-73.85)	(-33.99)	(-76.47)	(-32.14)	(-14.73)
		DI	-90.96	-59.55	-98.59	-61.25	-62.71
			(-83.42)	(-53.66)	(-92.30)	(-56.63)	(-36.37)
		TR	-90.94	-59.22	-94.41	-61.42	-61.45
			(-83.44)	(-53.56)	(-92.31)	(-56.53)	(-42.46)
		TE	-90.65	-59.62	-98.32	-61.06	-62.63
			(-83.44)	(-53.60)	(-92.45)	-65.61)	(-36.34)
Fe^{3+} / Fe^{2+}	+0.77	MO	-28.37	-31.89	-35.39	-41.98	-30.88
			(-25.30)	(-27.71)	(-33.30)	(-33.83)	(-8.08)
		DI	-38.43	-51.91	-49.12	-66.54	-52.56
			(-34.87)	(-47.39)	(-49.12)	(-58.33)	(-66.54)
		TR	-38.41	-51.58	-47.43	-66.72	-51.30
			(-34.88)	(-47.29)	(-49.13)	(-58.23)	(-35.81)
		TE	-38.12	-51.98	-51.34	-66.36	-52.48
			(-34.89)	(-47.32)	(-49.27)	(-67.30)	(-29.70)
Cu^{2+} / Cu^{+}	+0.15	MO	21.27	5.85	10.93	-3.42	-10.66
			(31.21)	(12.87)	(19.91)	(2.57)	(0.08)
		DI	11.21	-14.17	-2.80	-27.99	-32.34
			(21.65)	(-6.80)	(4.09)	(-21.93)	(-27.99)
		TR	11.23	-13.83	-1.11	-28.16	-31.08
			(21.63)	(-6.70)	(4.08)	(-21.83)	(-27.65)
		TE	11.52	-14.24	-5.02	-27.80	-32.26
			(21.63)	(-6.74)	(3.94)	(-30.91)	(-21.54)
Ti^{4+} / Ti^{3+}	0.00	MO	-22.27	14.91	-22.77	17.23	2.85
			(-15.93)	(19.41)	(-18.38)	(20.24)	(40.94)
		DI	-32.33	-5.11	-36.50	-7.34	-18.83
			(-25.50)	(-0.26)	(-34.20)	(-4.26)	(-7.34)
		TR	-32.31	-4.77	-34.81	-7.51	-17.57
			(-25.51)	(-0.16)	(-34.22)	(-4.16)	(13.21)
		TE	-32.02	-5.17	-38.72	-7.15	-18.75
			(-25.52)	(-0.20)	(-34.36)	(-13.23)	(19.32)
V^{3+} / V^{2+}	-0.26	MO	-17.58	12.50	-17.57	15.71	7.57
			(-7.88)	(17.01)	(-9.04)	(19.07)	(27.89)
		DI	-27.64	-7.53	-33.80	-8.85	-14.11
			(-17.44)	(-2.66)	(-24.86)	(-5.43)	(6.25)
		TR	-27.62	-7.19	-29.61	-9.02	-12.85
			(-17.46)	(-2.56)	(-24.88)	(-5.33)	(0.16)
		TE	-27.33	-7.59	-33.52	-8.66	-14.03
			(-17.46)	(-2.60)	(-25.01)	(-14.41)	(6.27)
Ti^{3+} / Ti^{2+}	-0.37	MO	7.93	33.06	20.55	47.59	34.19
			(19.95)	(38.89)	(17.66)	(52.90)	(45.98)
		DI	-2.13	13.03	6.81	23.03	12.51
			(10.38)	(19.22)	(1.83)	(28.40)	(23.03)
		TR	-2.11	13.37	8.51	22.85	13.77

			(10.37)	(19.32)	(1.82)	(28.50)	(18.25)
		TE	-1.82	12.97	4.59	23.22	12.59
			(10.37)	(19.28)	(1.68)	(19.43)	(24.36)
Cr^{3+} / Cr^{2+}	-0.41	MO	-43.87	-8.68	-43.87	-4.69	-37.20
			(-37.48)	(-2.56)	(-37.67)	(0.91)	7.61
		DI	-53.93	-28.70	-60.10	-29.26	-58.89
			(-47.05)	(-22.23)	(-53.50)	(-23.59)	(-14.03)
		TR	-53.91	-28.37	-55.91	-29.44	-57.63
			(-47.06)	(-22.13)	(-53.51)	(-23.49)	(-20.12)
		TE	-53.63	-28.77	-59.82	-29.07	-58.81
			(27.28)	(-22.17)	(-53.65)	(-32.57)	(-14.01)
In^{3+} / In^{2+}	-0.49	MO	22.05	27.61	26.28	32.83	31.96
			(27.65)	(32.20)	(29.95)	(35.97)	35.18
		DI	11.99	7.58	12.54	8.26	10.27
			(18.08)	(12.53)	(14.13)	(11.47)	(8.26)
		TR	12.01	7.92	14.24	8.08	11.54
			(18.07)	(12.63)	(14.12)	(11.57)	(7.45)
		TE	12.30	7.52	10.33	8.45	10.35
			(18.06)	(12.59)	(13.98)	(2.49)	(13.57)

[a] The MCP NoSeC VTZP core potential was applied for metals while all-electron Pople-style basis set was applied for carbon, chlorine and hydrogen.

[b] The LANL2DZ pseudopotential was applied for metals while all-electron Pople-style basis set was used for carbon, chlorine and hydrogen.

What is also apparent, is the fact that the analysis of the results gathered in table 3 and also the diagrams in figures 3 and 4 revealed that in the case of chromium salt at all levels of theory (at HF and DFT methods levels of theory and with the use of all types basis sets) the one-electron reduction of Cr^{3+} is always driven thermodynamically, in spite of the fact that the standard redox potential for this reduction is significantly negative. When calculated in gas phase (without PCM applied) the value of the relative energy at all levels of theory amounts to about 20 kcal/mol and is a little lower when the PCM is applied, except for the LANL2DZ pseudopotential and B3LYP functional where the energy calculated additionally with the use of the PCM is above 40 kcal/mol lower. Therefore, in order to avoid doubts in this case we calculated the thermodynamical barrier with the use of the MCP basis set and the B3LYP functional in the same manner. The energy amounts to -8.28 kcal/mol when calculated without PCM and -12.35 kcal/mol when the PCM was additionally applied. These new results indicate that the aberration in the case of Cr^{3+} reduction does not relate to the problem of the theory level, but is rather referred to the nature of the chromium III oxidizer in the one-electron reduction. One can conclude that in the case of chromium III chloride the reaction should indeed be observed.

For the first-step reduction of metal salts by di-p-xylylene (the dimer) ΔH and ΔG were estimated for the temperature T = 298.15 K and for the pressure P = 1013 hPa. After the calculation of partition-function contributions they were added to ΔE. The computations were performed by means of the DFT method with the BHHLYP functional and the MCP basis set on metal and 6-31G(d) basis set on all other atoms. It can be noted that inclusion of vibrational and rotational contributions to ΔH and ΔG is insignificant in comparison to energy barriers (see table 4). Consequently, the qualitative relations between ΔH and ΔG and the previously calculated ΔE (see table 3) remain the same for the reactions. It is therefore obvious that the largest energy component in these reactions is revealed in the electronic structure change. Similar effect was observed in theoretical studies of one-electron reduction of triplet-state oxygen molecule [68].

The computations of relative energies of transition metal cation redox half-reactions are

Table 4. Partition-function contributions to ΔH and to ΔG of the first-step one-electron reduction of metal salts by means of biradical di-p-xylylene (the dimer) and the values of ΔH and ΔG of these reactions calculated using the DFT method wth the BHHLYP functional and the MCP basis set on metal and 6-31G(d) basis set on other atoms.

$Me^{n+}/Me^{(n-1)+}$	$\Delta H_{rot,osc}$	$\Delta G_{rot,osc}$	ΔH	ΔG
Ag^{2+}/Ag^{+}	2.5	4.5	-54.45	-52.45
Co^{3+}/Co^{2+}	1.9	5.7	-55.57	-51.77
Mn^{3+}/Mn^{2+}	2.2	3.4	-54.42	-53.22
Fe^{3+}/Fe^{2+}	2.5	4.7	-55.83	-53.63
Cu^{2+}/Cu^{+}	1.2	1.4	-20.73	-20.53
Ti^{4+}/Ti^{3+}	1.9	1.0	-2.36	-3.26
V^{3+}/V^{2+}	1.9	4.2	-3.52	-1.22
Ti^{3+}/Ti^{2+}	1.6	4.1	30.00	32.50
Cr^{3+}/Cr^{2+}	1.9	2.0	-21.69	-21.59
In^{3+}/In^{2+}	2.0	2.3	13.47	13.77

typically subject to a large uncertainty[69]. On the other hand our model involves whole reaction energies, where the oxidation half-reaction regards radical parylene chains ionization and one shouldn't simply compare them with energies of half-reaction reductions of $Me^{n+}/Me^{(n-1)+}$ electrode in comparison to the reference standard hydrogen electrode But, to check, whether the MCP basis sets and the DFT method might work properly with the reduction/oxidation, we checked the Fe^{2+} ionization potential (IP) and it appeared that the consistency with experimental value (30.457 eV) is very good. Namely the calculated IP equals 30.866 eV, which ragards 0 K conditions but it's obvious that thermal contribution will not affect it much, as for the single atom there ar not vibrations and rotations, and eventually translations might change something, but they exclude at both sides because before and after the reaction we still have one atom.

Having analyzed the results in diagrams in figures 3 and 4, one can conclude that within some domain in the positive band of standard redox potential the dependence between the potential and the thermodynamical barrier of an appropriate reaction seems to be monotonous. As opposed to this, when the potential is negative then there are some aberrances. Namely in the case of chromium the results indicate that the product should be stable, while in the case of indium the one-electron reduction should not occur, but for these two cases the standard redox potential is negative and its value is similar. In these cases the feasibility of the reaction hangs on other factors, not on the difference between potentials. On the other hand, a look at the dependence between the potential and the calculated barriers for more positive (less negative) values of standard potential provides a conclusion that within some scope radical chains of parylene can behave like reductors.

Methods comparison

We used several methods and basis sets in the computations. The reason of this was to compare their effectiveness and fitness in the following mechanisms calculations. As it can be seen in table 3 and also in diagrams in figure 5 the Hartree-Fock method gives significantly different thermodynamical barriers in comparison to those obtained at the DFT level for almost all metals studied, except for silver and indium where the values were similar (these are the peripheral metals in the investigations). A very large discrepancy was obtained for copper II chloride reduction, where the HF barriers are positive, in spite of the fact that the standard potential is positive and in the case of neighboring titanium IV and iron III chlorides the relative energies are negative. Therefore, we decided not to use this method any longer in the calculations with the LANL2DZ pseudopotential (see table 3 and the diagrams in figure 5) as it seems to be insufficient even in comparison of the energetics of ground-state molecules.

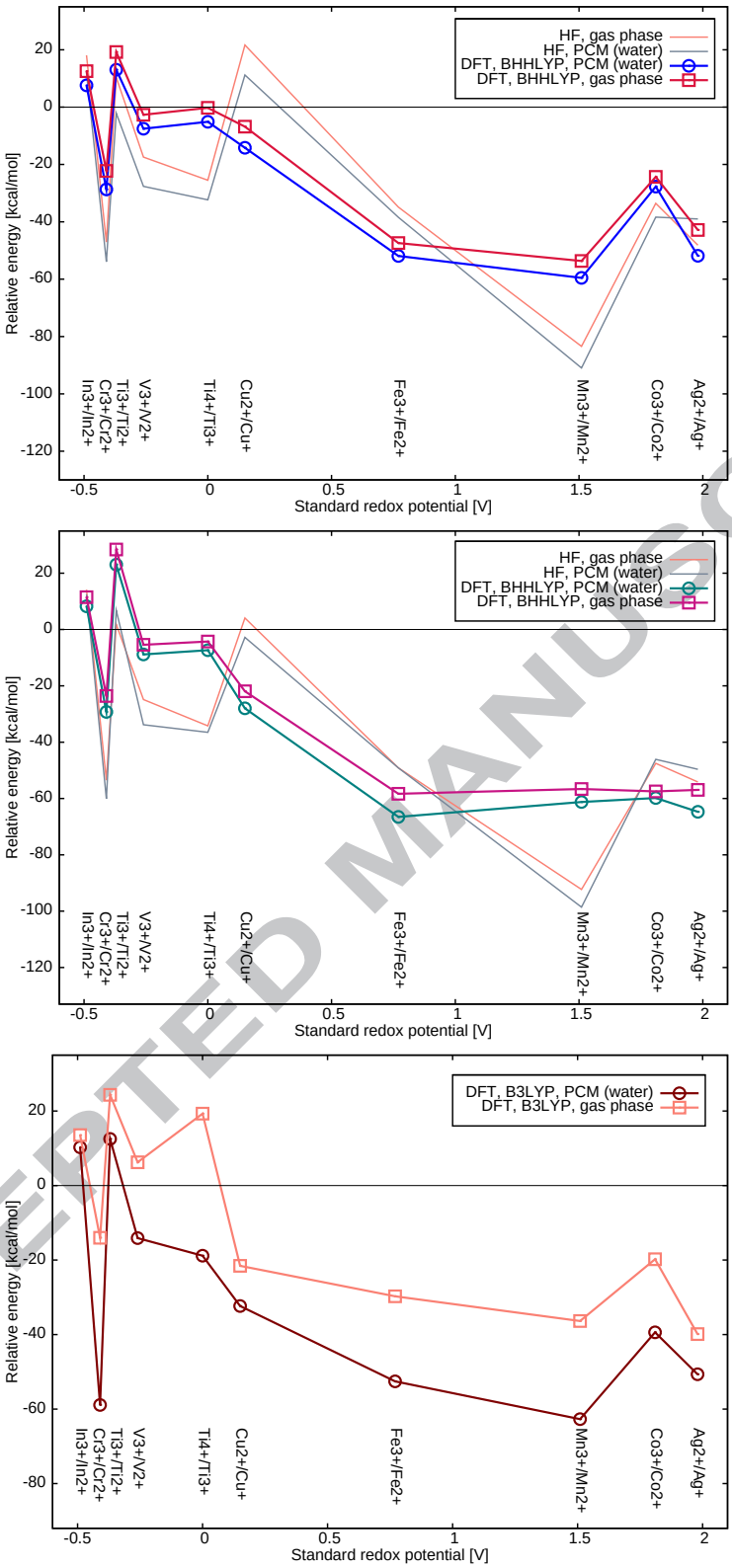

Figure 5. The comparison of thermodynamical barriers of first-step one-electron reduction by biradical di-p-xylylene. The Hartree-Fock energies are signified by thin lines, while the DFT energies are signified by thick lines.

Solvent presence, which was modeled by the PCM theory (the solvent chosen was water) influenced the ΔE in the way that decreased the energy relations by more or less constant value of energy where the higher value is for the gas phase reactions. But it is worth pointing out

that the effect of water existence in the solution is not so simple. One could imagine water molecules surrounding the cations and anions which obviously should influence the mechanism of the reduction. Moreover, the number of water molecules around cations should be different for different oxidation levels of the same metals and stechiometricity might be disturbed. Therefore, we resigned from the inclusion of solvent molecules in the calculations of energy effects in the redox reactions and applied the PCM instead.

Two-electron reduction

In order to check this, the two-electron reduction feasibility of some metal salts by the biradical parylene chains and by its monomers similar calculations for 3 reactions were also performed. However, it should be stated that from the geometrical point of view this type of reaction has lower significance. In accordance with the current knowledge on the polymerization mechanism of parylene, the chains of this kind of polymer grow by the propagation reaction by attachment of only one unit (one monomer) at a time to the radical end. If the two-electron reduction could occur then it means that two ends of the same chain should be involved in the reaction, but they are rather far away from each other. Also the two-electron transfer should occur simultaneously while in the case of linear chains it is less possible. Eventually, two-step one-electron reduction might take place, but the appropriate standard redox potentials for one-electron reductions should be positive. This in turn indicates a totally different mechanism. But in spite of this, even if this type of reactions does not take place, the thermodynamical barriers should manifest the feasibility of reduction of some oxidation agents by means of the radical chains. And this property of biradical parylene chains would be in this way well characterized, which in turn would endorse the theory on the one-electron reduction possibility in case of some metal salts.

Stechiometric notation of reactions studied is presented in figure 2. The reactions E and F correspond to the two-electron reduction where 2 chlorine atoms are transferred to p-xylylene molecule (reaction E) or to biradical linear chain of oligomers (reactions F). Similarly to the case of the second-step one-electron reduction the two-electron reduction leads to singlet-state closed-shell molecules with two chlorine atoms attached to their ends. In contrary to the first-step one-electron reduction case now the oligomers cannot take part neither in the polymerization nor in the next reduction.

The energetics of the two-electron reduction of metal salts by means of biradical oligomers and closed-shell p-xylylene (the monomer) are assembled in table 5. Three metals were chosen as the reactants and also in this case as in the case of one-electron reduction, the limitation was to choose only those metals for which the reduced product was still a cation.

In the case of the two-electron reduction of lead (see table 5) by means of biradical parylene chains the thermodynamical barriers are very low, ranging from -41 kcal/mol calculated at the Hartree-Fock method level and SBKJC basis set to -73.91 when calculated by means of the DFT method with the use of model core potential basis set. It is in very good agreement with the relatively high standard redox potential for the two electron reduction of Pb^{4+} which equals +1.67 V. For tin the thermodynamical barriers amount to about -9 kcal/mol when obtained with the use of the Hartree-Fock theory and the MCP basis and to about -25 kcal/mol when calculated with the use of the DFT method and BHHLYP functional and MCP basis set. In the case of the two-electron reduction of Sn^{4+} the standard redox potential amounts to +0.15 V. The thermodynamical barriers for the two-electron reduction of In^{3+} are much higher and amount to 6.76 kcal/mol when calculated by means of the ROHF method and the SBKJC pseudopotential and to about -18 kcal/mol when obtained by means of the DFT method and BHHLYP functional and the MCP basis set. When the PCM model was additionally applied the theromodynamical barriers decreased to about 10 kcal/mol at all levels of theory.

Also in this case, the reduction of metal salts by means of p-xylylene molecules (the monomers) is characterized by relatively high ΔE in comparison to the reactions with biradical reactants which indicate its much worse reactivity.

Table 5. DFT and Hartree-Fock relative energies (kcal/mol) of two-electron reduction by biradical di-p-xylylene (DPX) in gas phase.

$Me^{n+} / Me^{(n-1)+}$	E^0 [V]	S	HF SBKJC	RBHHLYP SBKJC	HF MCP[a] 6-31G(d)	RBHHLYP MCP[a] 6-31G(d)	UB3LYP LANL2DZ[b] 6-31+G(d)
Pb^{4+} / Pb^{2+}	+1.67	MO	-42.75	-36.21	-48.07	-55.60	-58.35
			(-30.38)	(-26.24)	(-40.11)	(-48.58)	(-37.64)
		DI	-53.89	-57.30	-64.87	-79.48	-81.05
			(-41.10)	(-47.05)	(-56.67)	(-73.91)	(-60.16)
		TR	-54.16	-57.53	-60.59	-86.26	-84.15
			(-41.24)	(-47.16)	(-61.04)	(-73.77)	(-60.08)
		TE	-53.95	-57.55	-68.63	-80.72	-76.25
			(-41.27)	-47.24	(-56.77)	(-81.65)	(-60.21)
Sn^{4+} / Sn^{2+}	+0.15	MO	-27.92	-24.52	-3.04	-8.39	-17.12
			(-13.09)	(-12.28)	(6.79)	(0.30)	(-3.22)
		DI	-39.07	-45.62	-19.85	-32.28	-39.81
			(-23.82)	(-33.08)	(-9.76)	(-25.03)	(-25.74)
		TR	-39.33	-45.85	-15.56	-39.06	-42.92
			(-23.95)	(-33.19)	(-14.13)	(-24.89)	(-25.67)
		TE	-39.13	-45.87	-23.61	-33.52	-35.02
			(-23.99)	-33.27	(-9.86)	(-32.78)	(-25.79)
In^{3+} / In^{+}	-0.44	MO	7.47	-0.66	6.36	2.22	8.59
			(17.48)	(8.26)	(12.49)	(7.45)	(12.57)
		DI	-3.68	-21.76	-10.45	-21.67	-14.11
			(6.76)	(-12.54)	(-4.07)	(-17.88)	(-9.95)
		TR	-3.94	-22.00	-6.16	-28.45	-17.35
			(6.62)	(-12.65)	(-8.44)	(-17.74)	(-9.88)
		TE	-3.74	-22.01	-14.21	-22.91	-9.31
			(6.59)	-12.73	(-4.17)	(-25.63)	(-10.00)

[a] The MCP NoSeC VTZP core potential was applied for metals while all-electron Pople-style basis set was applied for carbon, chlorine and hydrogen.

[b] The LANL2DZ pseudopotential was applied for metals while all-electron Pople-style basis set was used for carbon, chlorine and hydrogen.

As in the case of the one-electron reduction of metal salts the thermodynamical barriers decrease only when the standard redox potential increases. This in turn reveals the reductive nature of biradical oligomers also in these hypothetical two-electron reductions.

Conclusions

Stechiometric reactions of the one-electron reduction of metal salts by radical chains of parylene were proposed. Although the mechanism of the reduction is yet unknown, the analysis of thermo-dynamical barriers reveals very clearly that biradical dimers, trimers, tetramers and most likely each biradical chain of parylene have reductive nature. They have therefore the power to reduce metal salts if only the standard redox potential of appropriate half reaction is sufficiently high. Moreover, the p-xylylene monomers which in the first phases of parylene's CVD adhere to the surface of solid or liquid (in this case the polarity plays a role) are relatively less capable of reacting in this way. This, in turn is in good agreement with the recently found lower reactivity of quinoidal p-xylylene molecules with variously substituted vinyl molecules in comparison to the reactivity of p-xylylene dimer [22]. The relation regarded not only the

thermodynamical barriers but also the kinetic barriers. Our results reveal that the one-electron reduction thermodynamical barriers are lower than zero in the cases where the standard redox potential of the reduction half reaction for metal is higher than zero and generally increase when the potential decresases, which in turn indicates lower feasibility of the reactions. This is also in good agreement with a typical scenario of a redox reaction. In such cases the significance of only half reaction standard potential is not sufficient but one requires also the second half reaction potential. Comparing just these two values can give an answer on the feasibility of the redox reaction. In the case of the two-electron reduction which is much less probable, the reductive nature of biradical chains of parylene was also significantly manifested, and we are now confident that the one-electron reduction of metal salts, even in two steps reactions can be considered possible. The calculations also lead to an assumption that the standard redox potential for the reduction of biradical chains of parylene is lower than zero at the standard electrode potential series.

It should also be noted at the end that, as Vaeth et all [25] found and Lahann and coworkers confirmed [27], pure metals are also capable of quenching of the polymerization of parylene. Our results revealed reductive nature of parylene chains in reactions with some metal salts but even so the stechiometric notation analogous to these reactions should not be used for metals. On the other hand, it does not exclude the possibility of the SOMO electrons engagement in the reactions with metals; on the contrary, it seems very probable that a counterpart of the reduction is also responsible for quenching of radical-driven polymerizations by means of metals.

Acknowledgements

This work was supported by the STREP n°033201 funded by the European Commission under the sixth Framework Programme, by the grant from the Polish Ministry of Science and Education (399/6PRUE/2007/7) as well as by the grant NMP4-SL-2010-246362 under the seventh Framework Programme. Calculations were carried out at the supercomputers of Informatics Center of the Metropolitan Academic Network (IC MAN) at the Gdansk University of Technology in Poland.

References

[1] H. Keppner, M. Benkhaira, Patent: Method for producing a plastic membrane device and the thus obtained device. WO 2006/063955.

[2] N. Binh-Khiem, K. Matsumoto, I. Shimoyama, Tensile film stress of parylene deposited on liquid., Langmuir 26 (24) (2010) 18771–18775.

[3] M. Szwarc, Some remarks on the $CH_2C_6H_4CH_2$ molecule., Faraday Soc. 2 (1947) 46–49.

[4] W. F. Gorham, A new general synthetic method for preparation of linear poly-p-xylylenes., J. Polym. Sci. Polym. Chem. 4 (1966) 3027–3039.

[5] L. A. Errede, M. Szwarc, Chemistry of p-xylylene, its analogues, and polymers., Q. ReV. 12 (1958) 301–320.

[6] W. F. Gorham, Para-xylylene polymers, US Patent 3,342,754 (1967).

[7] J. Lahann, T. Rodon, H. Lu, M. Balcells, K. F. Jensen, R. Langer, Reactive polymer coatings: A first step towards surface engineering of microfluidic devices.., Anal. Chem. 75 (2003) 2117–2122.

[8] S. Takayama, E. Ostuni, P. LeDuc, K. Naruse, D. E. Ingber, G. M. Whitesides, Subcellular positioning of small molecules., Nature 411 (2001) 1016–1016.

[9] G. Applerot, R. Abu-Mukh, A. Irzh, J. Charmet, H. Keppner, E. Laux, G. Guibert, A. Gedanken, Decorating parylene-coated glass with ZnO nanoparticles for antibacterial applications: A comparative study of sonochemical, microwave, and microwave-plasma coating routes., Appl. Mat. Interf. 2 (4) (2010) 1052–1059.

[10] W. F. Beach, C. Lee, D. R. Bassett, T. M. Austin, R. Olson, ,,Xylylene Polymers" in Encyclopedia of Polymer Science and Technology, 3rd ed., 2004.

[11] A. Kahouli, A. Sylwestre, L. Ortega, F. Pomni, B. Yangui, M. Maillard, B. Berge, J.-C. Robert, J. Legrand, Structural and dielectric study of parylene C thin films., App. Phys. Lett., 94 (2009) 152901–152903.

[12] A. Nosal, A. Izydorczyk, A. Sobczyk-Guezenda, L. Guchowski, H. Szymanowski, M. Gazicki-Lipman, Parylene coatings on biological specimens., J. Achiev. Mat. Manufact. Eng. 37 (2009) 442–447.

[13] W. F. Beach, H. F. Mark (Ed.), Encyclopedia of Polymer Science and Technology., New York, 2004.

[14] H. Hopf, [2.2]paracyclophanes in polymer chemistry and materials science., Angew. Chem. Int. Ed. 47 (2008) 9808–9812.

[15] S. Iwatsuki, M. Kubo, T. Kumeuchi, New method for preparation of poly(phenylene-vinylene) film., Chem. Lett. 20 (7) (1991) 1071–1074.

[16] E. G. J. Staring, D. Braun, G. L. J. A. Rikken, R. J. C. E. Demandt, Y. A. R. R. Kessener, M. Bauwmans, D. Broer, Chemical vapor deposition of poly(1,4-phenylenevinylene) films., Synth. Met. 67 (1994) 71–75.

[17] J. Lahann, Vapor-based polymer coatings for potential biomedical applications., Polym. Int. 55 (2006) 1361–1370.

[18] M. Cetinkaya, N. Malvadkar, M. C. Demirel, Power-law scaling of structured poly(p-xylylene) films deposited by oblique angle., J. Polym. Sci. Pt. B: Polym. Phys. 46 (2008) 640–648.

[19] A. Bolognesi, C. Botta, A. Andicsova, U. Giovanella, S. Arnautov, J. Charmet, E. Laux, H. Keppner, Chemical binding of unsaturated fluorenes to poly(2-chloroxylylene) thin films., Macromol. Chem. Phys. 210 (2009) 2052–2057.

[20] M. Naddaka, F. Asen, S. Freza, M. Bobrowski, P. Skurski, E. Laux, J. Charmet, H. Keppner, M. Bauer, J.-P. Lellouche, Functionalization of parylene during its chemical vapour deposition., J. Polym. Sci. Part A 49 (2011) 2952–2958.

[21] S. Freza, P. Skurski, M. Bobrowski, Influence of substituents in vinyl groups on reactivity of parylene during polymerization process., Chem. Phys. 368 (2010) 126–132.

[22] M. Bobrowski, S. Freza, P. Skorski, The electronic structure of p-xylylene and its reactivity with vinyl molecules., Chem. Phys. 382 (2011) 20–26.

[23] H. Reiss, Homogeneous gas phase polymerization., Acc. Chem. Res. 30 (1997) 297–305.

[24] M. Cetinkaya, S. Boduroglu, M. C. Demirel, Growth of nanostructured thin films of poly(p-xylylene) derivatives by vapor deposition., Polymer 48 (2007) 4130–4134.

[25] K. M. Vaeth, K. F. Jensen, Transition metals for selective chemical vapor deposition of parylene-based polymers., Chem. Mater. 12 (2000) 1305–1313.

[26] M. C. Demirel, Emergent properties of spatially organized poly(p-xylylene) films fabricated by vapor deposition, Coll. and Surf. A: Physicochem. Eng. Asp. 321 (2008) 121–124.

[27] K. Y. Suh, R. Langer, J. Lahann, Fabrication of elastomeric stamps with polymer-reinforced sidewalls via chemically selective vapor deposition polymerization of poly p-xylylene., Appl. Phys. Lett. 83 (20) (2003) 4250–4252.

[28] Y. Elkasabi, M. Yoshida, H. Nandivada, H.-Y. Chen, J. Lahann, Towards multipotent coatings: Chemical vapor deposition and biofunctionalization of carbonyl-substituted copolymers., Macromol. Rapid Commun. 29 (2008) 855–870.

[29] A. V. Vasenkov, Atomistic modeling of parylene-metal interactions for surface microstructuring, J. Mol. Model. 17 (12) (2011) 3219–3228.

[30] A. Y. Olenin, G. V. Lisichkin, Metal nanoparticles in condensed media: preparation and the bulk and surface structural dynamics, Russian Chemical Reviews 80 (7) (2011) 605–630.

[31] P. Neta, R. E. Huie, Free-radical chemistry of sulfite, Env. Health Persp. 64 (1985) 209–217.

[32] D. Pramanick, S. R. Palit, Ferrous-bromate redox as initiator of aqueous vinyl polymerization, Kolloid-Zeitschrift und Zeitschrift fur Polymere 229 (1) (1968) 24–28.

[33] V. Niemi, P. Knuuttila, J.-E. Ästerholm, J. Korvola, Polymerization of 3-alkylthiophenes with $FeCl_3$., Polymer 33 (7) (1992) 1559–1562.

[34] J. B. Fortin, T. M. Lu, A model for the chemical vapor deposition of poly(p-xylylene) (parylene) thin films., Chem. Mater. 14 (2002) 1945–1949.

[35] W. Bowie, Y. P. Zhao, Monte carlo simulation of vapor deposition polymerization., Surf. Sci. 563 (2004) L245–L250.

[36] K. Smalara, A. Gieldon, M. Bobrowski, J. Rybicki, C. Czaplewski, Theoretical study of polymerization mechanism of p-xylylene based polymers., J. Phys. Chem. A 114 (2010) 4296–4303.

[37] A. D. Becke, A new mixing of Hartree-Fock and local density-functional theories., J. Chem. Phys. 98 (1993) 1372–1377.

[38] A. D. Becke, Density-functional thermochemistry. III. the role of exact exchange., J. Chem. Phys. 98 (1993) 5648–5642.

[39] P. J. Stephens, F. J. Devlin, C. F. Chabalowski, M. J. Frisch, Ab initio calculation of vibrational absorption and circular dichroism spectra using density functional force fields., J. Phys. Chem. 98 (1994) 11623–11627.

[40] R. H. Hertwig, W. Koch, On the parameterization of the local correlation functional. what is Becke-3-LYP?, Chem. Phys. Lett. 268 (1997) 345–351.

[41] S. Saini, B. M. Deb, A computational study of the interaction of [7]-helicene with alkali cations and benzene., Indian J. Chem. 46A (2007) 9–15.

[42] A. K. Pathak, T. Mukherjee, D. K. Maity, Quantum chemical study on UV-vis spectra of microhydrated iodine dimer radical anion., J. Phys. Chem. A 114(2) (2010) 721–724.

[43] A. Heelmann, G. Jansen, First-order intermolecular interaction energies from Kohn-Sham orbitals., Chem. Phys. Lett. 357 (2002) 464–470.

[44] W. J. Hehre, R. Ditchfield, J. A. Pople, Self-consistent molecular orbital methods. XII. further extensions of Gaussian-type basis sets for use in molecular orbital studies of organic molecules., J. Chem. Phys. 56 (1972) 2257–2261.

[45] R. Ditchfield, W. J. Hehre, J. A. Pople, Self-consistent molecular orbital methods. 9. extended Gaussian-type basis for molecular-orbital studies of organic molecules., J. Chem. Phys. 54 (1971) 724–728.

[46] M. M. Francl, W. J. Pietro, W. J. Hehre, J. S. Binkley, D. J. DeFrees, J. A. Pople, M. S. Gordon, Self-consistent molecular orbital methods. 23. a polarization-type basis set for 2nd-row elements., J. Chem. Phys. 77 (1982) 3654–3665.

[47] M. J. Frisch, A. J. Pople, J. S. Binkley, Self-consistent molecular orbital methods. 25. supplementary functions for Gaussian basis sets., J. Chem. Phys. 80 (1984) 3265–3269.

[48] W. J. Stevens, H. Basch, M. Krauss, Compact effective potentials and efficient shared-exponent basis-sets for the 1st-row and 2nd-row atoms., J. Chem. Phys. 81 (1984) 6026–6033.

[49] W. J. Stevens, M. Krauss, H. Basch, P. G. Jasien, Relativistic compact effective potentials and efficient, shared-exponent basis-sets for the 3rd-row, 4th-row, and 5th-row atoms., Can. J. Chem. 70 (1992) 612–630.

[50] T. R. Cundari, W. J. Stevens, Effective core potential methods for the lanthanides., J. Chem. Phys. 98 (1993) 5555–5565.

[51] P. J. Hay, W. R. Wadt, Ab initio effective core potentials for molecular calculations - potentials for the transition-metal atoms Sc to Hg., J. Chem. Phys. 82 (1985) 270–83.

[52] W. R. Wadt, P. J. Hay, Ab initio effective core potentials for molecular calculations - potentials for main group elements Na to Bi., J. Chem. Phys. 82 (1985) 284–98.

[53] P. J. Hay, W. R. Wadt, Ab initio effective core potentials for molecular calculations - potentials for K to Au including the outermost core orbitals., J. Chem. Phys. 82 (1985) 299–310.

[54] Y. Osanai, M. S. Mon, T. Noro, H. Mori, H. Nakashima, M. Klobukowski, E. Miyoshi, Revised model core potentials for second-row transition metal atoms from Y to Cd., Chem. Phys. Lett. 452 (2008) 210–214.

[55] T. Noro, M. Sekiya, T. Koga, H. Matsuyama, Valence and correlated basis sets for the first transition atoms from Sc to Zn., Theor. Chem. Acc. 104 (2000) 146–152.

[56] Y. Osanai, E. Soejima, T. Noro, H. Mori, M. M. San, M. Klobukowski, E. Miyoshi, Revised model core potentials for second-row transition metal atoms from Y to Cd., Chem. Phys. Lett. 463 (2008) 230–234.

[57] Y. Osanai, M. Sekiya, T. Noro, T. Koga, Valence and correlating basis sets for the second transition-metal atoms from Y to Cd., Mol. Phys. 101 (2003) 65–71.

[58] E. Miyoshi, Y. Sakai, K. Tanaka, M. Masamura, Relativistic dsp-model core potentials for main group elements in the fourth, fifth, and sixth rows and its applications., J. Mol. Struct. (THEOCHEM) 451 (1998) 73–79.

[59] M. Sekiya, T. Noro, Y. Osanai, T. Koga, Contracted polarization functions for the atoms Ca, Ga-Kr, Sr, and In-Xe., Theor. Chem. Acc. 106 (2001) 297–300.

[60] T. Noro, M. Sekiya, Y. Osanai, E. Miyoshi, T. Koga, Relativistic correlating basis sets for the main group elements from Cs to Ra., J. Chem. Phys. 119 (2003) 5142–5148.

[61] M. W. Schmidt, K. K. Baldridge, J. A. Boatz, S. T. Elbert, M. S. Gordon, J. J. Jensen, S. Koseki, N. Matsunaga, K. A. Nguyen, S. Su, T. L. Windus, M. Dupuis, J. A. Montgomery, General atomic and molecular electronic structure system., J. Comput. Chem. 14 (1993) 1347–1363, GAMESS version from 12 JAN 2009 (R3).

[62] M. J. Frisch, G. W. Trucks, H. B. Schlegel, G. E. Scuseria, M. A. Robb, J. R. Cheeseman, J. A. Montgomery, Jr., T. Vreven, K. N. Kudin, J. C. Burant, J. M. Millam, S. S. Iyengar, J. Tomasi, V. Barone, B. Mennucci, M. Cossi, G. Scalmani, N. Rega, G. A. Petersson, H. Nakatsuji, M. Hada, M. Ehara, K. Toyota, R. Fukuda, J. Hasegawa, M. Ishida, T. Nakajima, Y. Honda, O. Kitao, H. Nakai, M. Klene, X. Li, J. E. Knox, H. P. Hratchian, J. B. Cross, V. Bakken, C. Adamo, J. Jaramillo, R. Gomperts, R. E. Stratmann, O. Yazyev, A. J. Austin, R. Cammi, C. Pomelli, J. W. Ochterski, P. Y. Ayala, K. Morokuma, G. A. Voth, P. Salvador, J. J. Dannenberg, V. G. Zakrzewski, S. Dapprich, A. D. Daniels, M. C. Strain, O. Farkas, D. K. Malick, A. D. Rabuck, K. Raghavachari, J. B. Foresman, J. V. Ortiz, Q. Cui, A. G. Baboul, S. Clifford, J. Cioslowski, B. B. Stefanov, G. Liu, A. Liashenko, P. Piskorz, I. Komaromi, R. L. Martin, D. J. Fox, T. Keith, M. A. Al-Laham, C. Y. Peng, A. Nanayakkara, M. Challacombe, P. M., Gaussian 03, Revision E.01., Wallingford CT, 2004.

[63] V. V. Zelentsov, G. M. Larin, E. V. Ivanov, N. V. Gerbeleu, A. V. Ablov, Equilibrium between low-spin and high-spin states in iron (III) complexes, Teoret. Eksper. Khim. 7 (6) (1970) 798–803.

[64] V. G. Bhide, D. S. Rajoria, G. R. Rao, C. N. R. Rao, Mossbauer studies of the high-spin - low-spin equilibria and the localized-collective electron transition in $LaCoO_3$, Phys. Rev. B 6 (3) (1972) 1021–1032.

[65] A. Vertes, Z. Kajcsos, L. Marczis, G. Brauer, J. Huller, I. Zay, K. Burger, Effect of the spin state of transition metals on their interaction with orthopositronium in aqueous solutions., J. Phys. Chem. 88 (1984) 3969–3971.

[66] J. Fleisch, P. Gutlich, K. M. Hasselbach, W. Muller, High spin-low spin transition in substituted phenanthroline complexes of iron (II)., J. de Phys. 35 (12) (1974) 659–662.

[67] V. S. Oganesyan, S. J. George, M. R. Cheesman, A. J. Thomson, A novel, general method of analyzing magnetic circular dichroism spectra and magnetization curves of high-spin metal ions: Application to the protein oxidized rubredoxin, Desulfovibrio gigas., J. Chem. Phys. 110 (2) (1999) 762–777.

[68] M. Bobrowski, A. Liwo, K. Hirao, Theoretical study of the energetics of the reactions of triplet dioxygen with hydroquinone, semiquinone, and their protonated forms: Relation to the mechanism of superoxide generation in the respiratory chain., J. Phys. Chem. B 111 (2007) 3543–3549.

[69] P. Jaque, A. V. Marenich, C. J. Cramer, D. G. Truhlar, Computational electrochemistry: The aqueous ru^{3+}—ru^{2+} reduction potential, J. Phys. Chem. C 111 (2007) 5783–5799.

Fig1

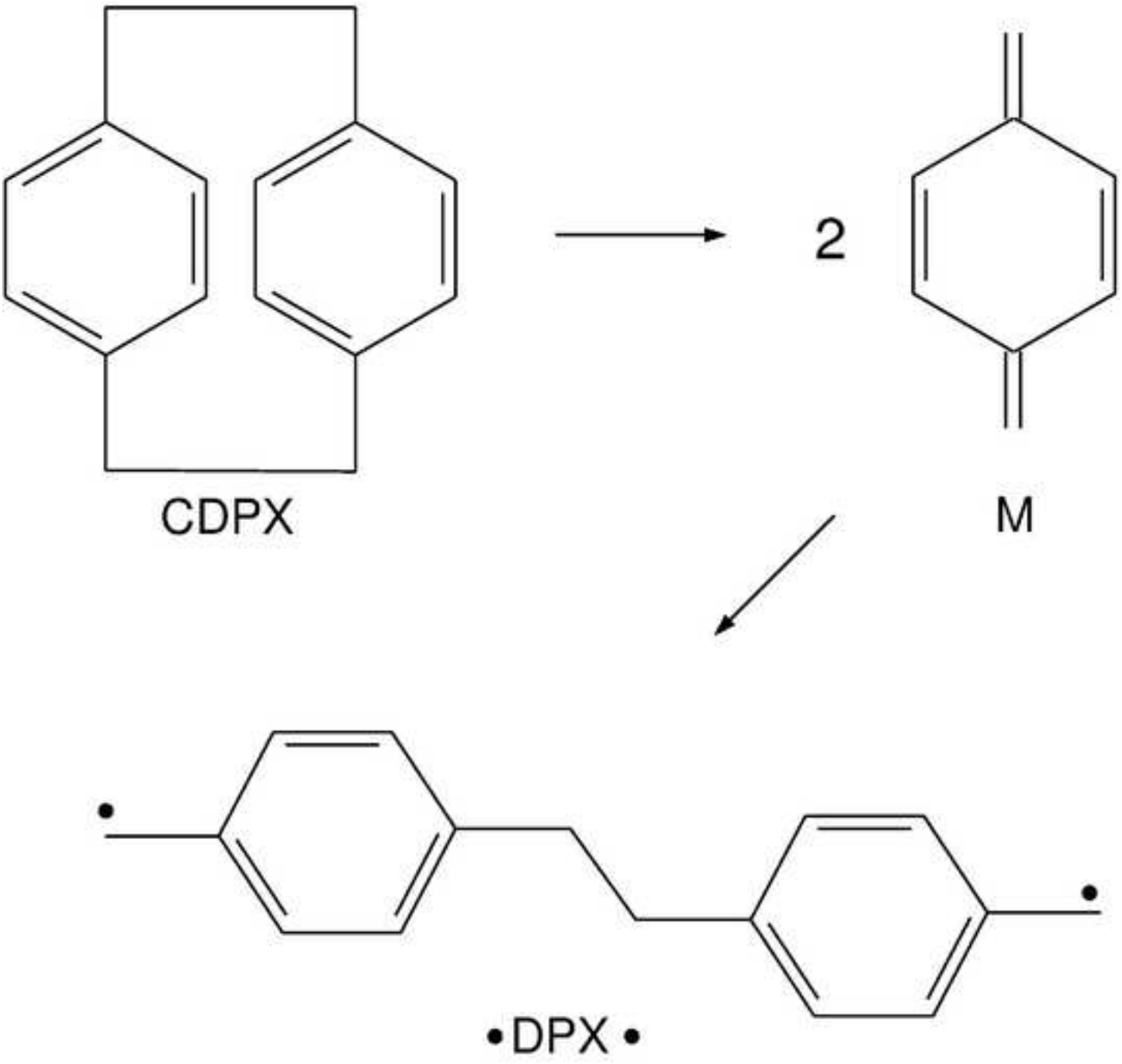

Fig2

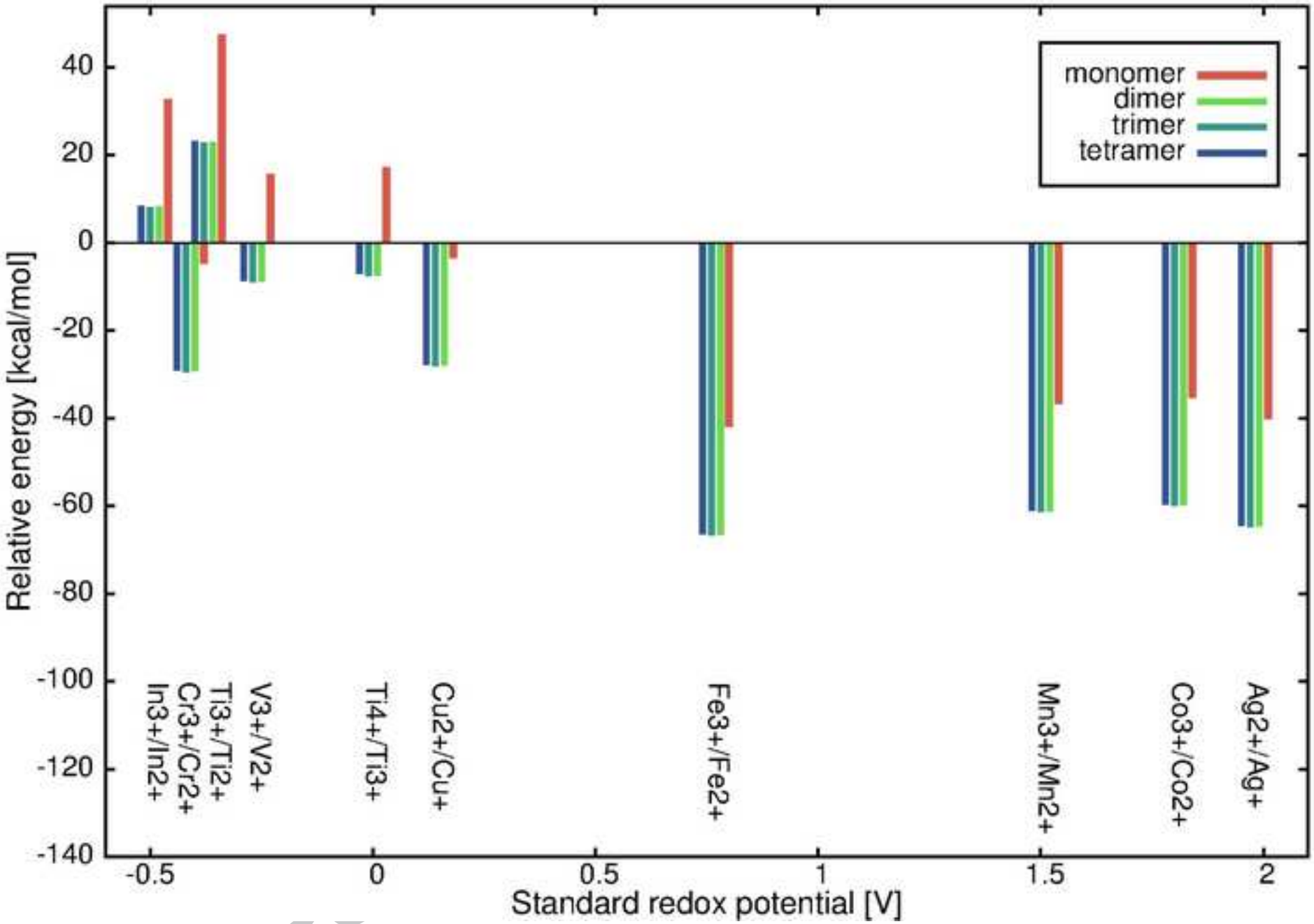

Fig3

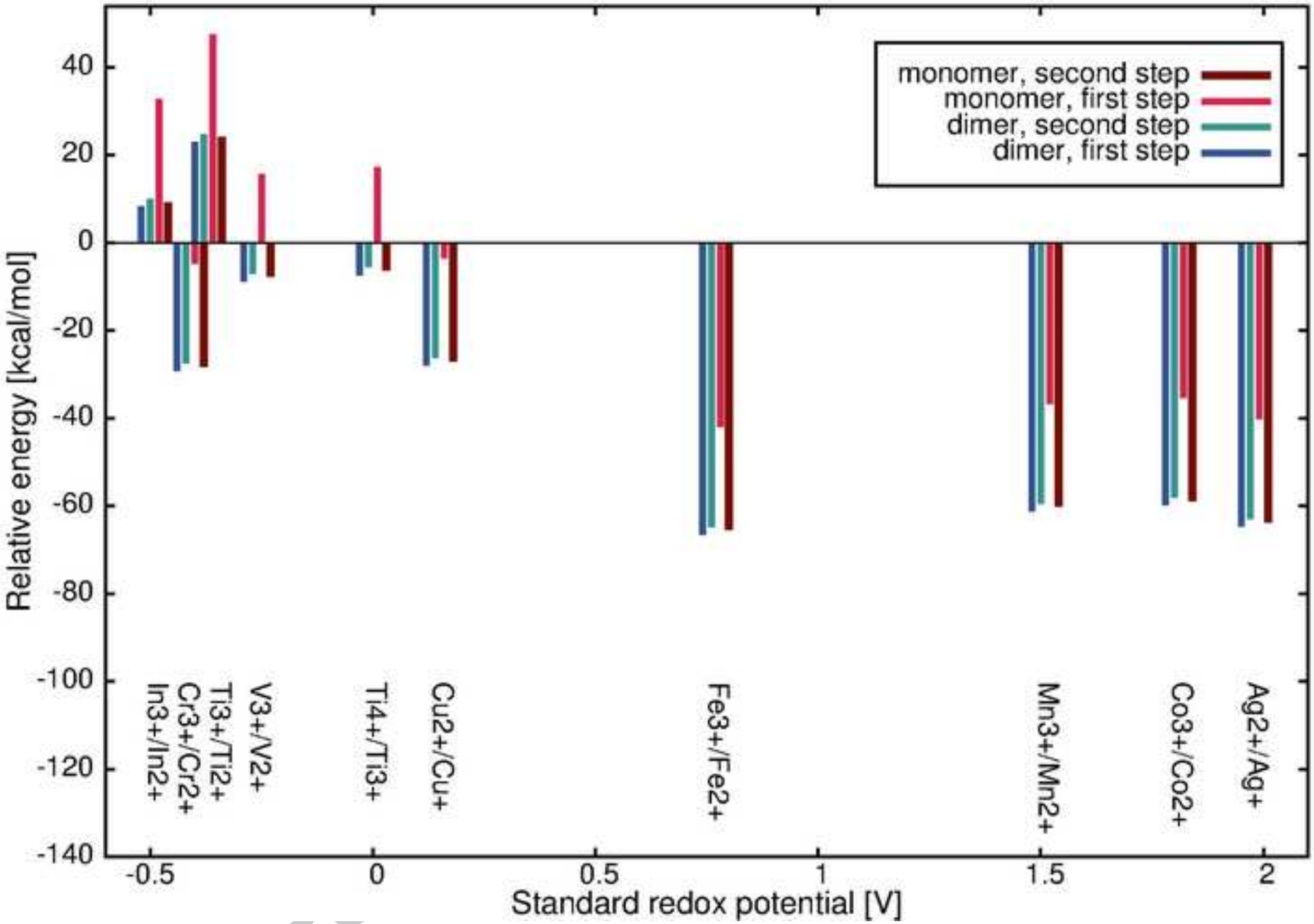

Fig4

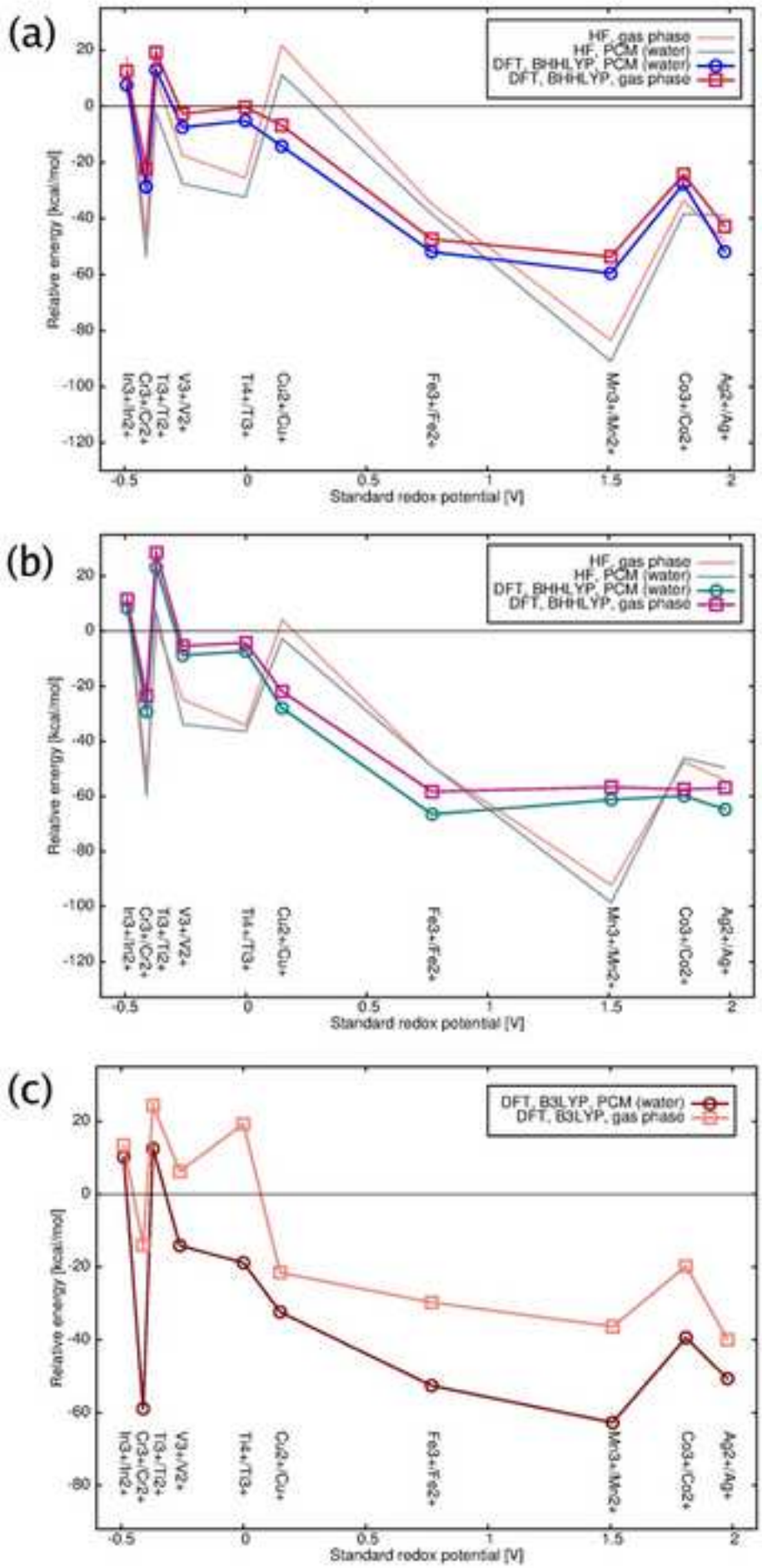

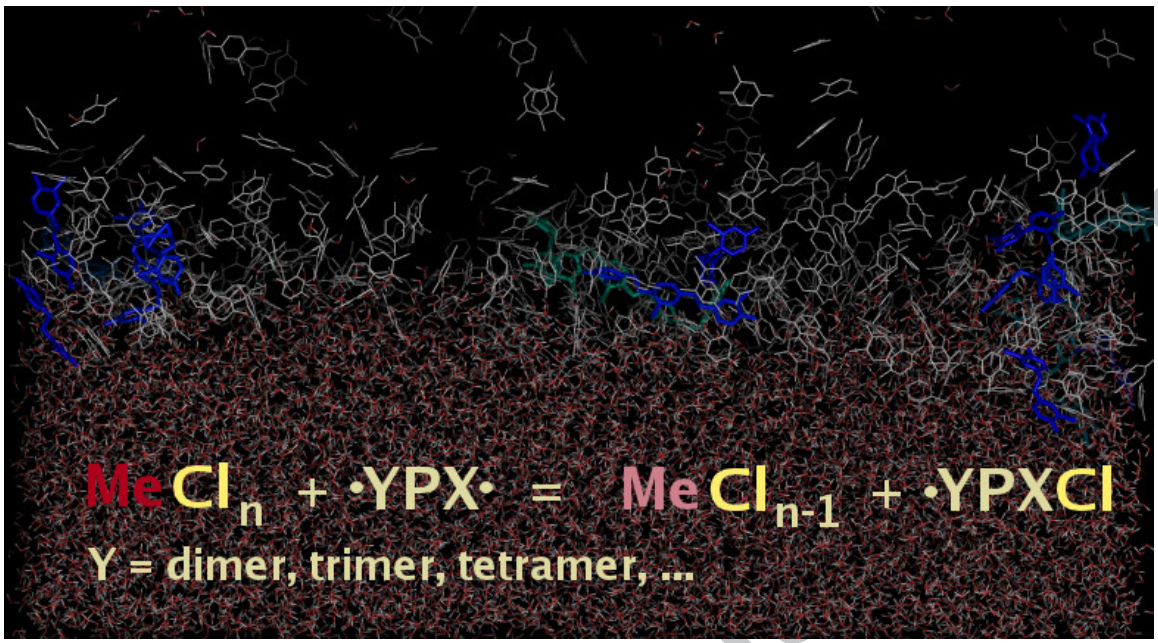

- Metal salts can quench the polymerization of poly-p-xylylens (parylenes).
- The reaction might go through the one-electron reduction of metal salt.
- The process can be a two-stage reduction leading to a complete quenching.
- Thermodynamical barriers are negative if the standard redox potential is negative.